The inferior olive is essential for long-term maintenance of a simple motor skill

Xiang Yang Chen,[1,2,3]* Yu Wang,[1,3]* Yi Chen,[1,3] Lu Chen,[1,3] and Jonathan R. Wolpaw[1,2,3,4]

[1]*National Center for Adaptive Neurotechnologies, Wadsworth Center, New York State Department of Health, Albany, New York;* [2]*Department of Biomedical Sciences, State University of New York, Albany, New York;* [3]*Albany Stratton Department of Veterans Affairs Medical Center, Albany, New York; and* [4]*Department of Neurology, Columbia University, College of Physicians and Surgeons, New York, New York*

Chen XY, Wang Y, Chen Y, Chen L, Wolpaw JR. The inferior olive is essential for long-term maintenance of a simple motor skill. *J Neurophysiol* 116: 1946–1955, 2016. First published August 17, 2016; doi:10.1152/jn.00085.2016.—The inferior olive (IO) is essential for operant down-conditioning of the rat soleus H-reflex, a simple motor skill. To evaluate the role of the IO in long-term maintenance of this skill, the H-reflex was down-conditioned over 50 days, the IO was chemically ablated, and down-conditioning continued for up to 102 more days. H-reflex size just before IO ablation averaged 62($\pm$2 SE)% of its initial value ($P < 0.001$ vs. initial). After IO ablation, H-reflex size rose to 75–80% over ~10 days, remained there for ~30 days, rose over 10 days to above its initial value, and averaged 140($\pm$14)% for the final 10 days of study ($P < 0.01$ vs. initial). This two-stage loss of down-conditioning maintenance correlated with IO neuronal loss ($r = 0.75$, $P < 0.01$) and was similar to the loss of down-conditioning that follows ablation of the cerebellar output nuclei dentate and interpositus. In control (i.e., unconditioned) rats, IO ablation has no long-term effect on H-reflex size. These results indicate that the IO is essential for long-term maintenance of a down-conditioned H-reflex. With previous data, they support the hypothesis that IO and cortical inputs to cerebellum combine to produce cerebellar plasticity that produces sensorimotor cortex plasticity that produces spinal cord plasticity that produces the smaller H-reflex. H-reflex down-conditioning appears to depend on a hierarchy of plasticity that may be guided by the IO and begin in the cerebellum. Similar hierarchies may underlie other motor learning.

operant conditioning; spinal cord; H-reflex; plasticity; sensorimotor cortex; cerebellum; memory; learning

NEW & NOTEWORTHY

This study shows that the inferior olive (IO) is essential for maintaining a down-conditioned H-reflex in rats. It supports the hypothesis that IO and cortical inputs to cerebellum combine to produce cerebellar plasticity that produces cortical plasticity that produces spinal cord plasticity that reduces the H-reflex. This simple motor skill appears to depend on a hierarchy of plasticity that is guided by the IO and begins in the cerebellum. Comparable hierarchies might underlie other skills.

MOTOR LEARNING DEPENDS on plasticity from the cortex to the spinal cord (e.g., Carrier et al. 1997; Lieb and Frost 1997;

Longley and Yeo 2014; Wolpaw and Lee 1989). An operantly conditioned change in the size of the H-reflex [an electrical analog of the spinal stretch reflex (e.g., the knee-jerk reflex)] is a simple motor skill (i.e., an adaptive behavior acquired through practice) that provides an excellent opportunity for determining how changes at multiple sites combine to account for the acquisition and maintenance of a new behavior. This skill involves plasticity in both the brain and the spinal cord (see for review Thompson and Wolpaw 2014; Wolpaw 2010; Wolpaw and Chen 2009). The fact that the brain and spinal cord are connected by well-defined and accessible pathways makes it possible to study how spinal and supraspinal plasticity interact to acquire and maintain a smaller (i.e., down-conditioned) or larger (i.e., up-conditioned) H-reflex.

Previous studies show that the corticospinal tract (CST), cerebellar output to cortex, and the inferior olive (IO) are essential for acquisition of the spinal cord plasticity that is directly responsible for a down-conditioned H-reflex; other major descending and ascending tracts are not needed (Chen et al. 2016; Chen and Wolpaw 1997, 2002, 2005; Wolpaw and Chen 2006). Furthermore, in rats that have already been down-conditioned, the H-reflex decrease disappears 5–10 days after CST transection vs. 40–50 days after ablation of the cerebellar output nuclei dentate and interpositus (DIN) (Chen and Wolpaw 2002; Wolpaw and Chen 2006). The difference in timing between the effects of CST and DIN lesions suggests that this simple skill depends on a hierarchy in which cerebral cortical plasticity that depends on the cerebellum guides and maintains the plasticity in the spinal cord that accounts for the smaller H-reflex (Wolpaw and Chen 2006).

The present study was motivated by these maintenance results and by current ideas as to the role of the cerebellum and IO in other simple motor skills (Boyden et al. 2004; Cheron et al. 2013; Freeman and Steinmetz 2011; Longley and Yeo 2014; Martin et al. 1996; Thompson 2005). It evaluated the role of the IO in the long-term maintenance of a down-conditioned H-reflex. Normal rats were down-conditioned over 50 days, the IO was ablated, and down-conditioning continued for up to 102 more days. The results extend previous findings and provide important new insight into the multisite plasticity that underlies this simple motor skill.

METHODS

The subjects were 14 young adult male Sprague-Dawley rats weighing 332($\pm$42 SD) g (range 284–419 g) at the beginning of

* X. Y. Chen and Y. Wang contributed equally to this work.

Address for reprint requests and other correspondence: X. Y. Chen, National Center for Adaptive Neurotechnologies, Wadsworth Center, New York State Dept. of Health, PO Box 509, Albany, NY 12201-0509 (e-mail: xiangyang.chen@health.ny.gov).

study. All procedures satisfied the *Guide for the Care and Use of Laboratory Animals* (National Academies Press, 2011) and had been approved by the Institutional Animal Care and Use Committee of the Wadsworth Center. The protocols for implantation of the nerve-stimulating cuff and EMG recording electrodes, M-response and H-reflex elicitation, H-reflex conditioning, data collection and analysis in freely moving rats, IO ablation, and histological evaluation have been fully described previously (Chen et al. 2016; Chen and Wolpaw 1995, 2002, 2005; Wolpaw and Chen 2006; Wolpaw and Herchenroder 1990). They are summarized here.

Electrode implantation. Each rat was deeply anesthetized and implanted with chronic stimulating and recording electrodes in the right hindlimb. To record soleus EMG activity, a pair of fine-wire electrodes was placed in the right soleus muscle. To elicit the soleus H-reflex, a nerve-stimulating cuff was placed on the right posterior tibial nerve just above the triceps surae branches. The Teflon-coated wires from the electrodes passed subcutaneously to a connector plug on the skull. Immediately after surgery, the rat was placed under a heating lamp and given an analgesic (Demerol, 0.2 mg im). Once awake, it received a second dose of analgesic and was returned to its cage. Rats recovered quickly and resumed their normal activity within 1–3 h.

H-reflex conditioning protocol and experimental design. Data collection began at least 20 days after electrode implantation and continued 24 h/day, 7 days/wk for up to 170 days (Fig. 1*A*). During this period, the rat lived in a standard rat cage with a 40-cm flexible cable attached to the skull plug. The cable allowed the animal to move freely about the cage; it carried the wires from the electrodes to a commutator above the cage that connected to an EMG amplifier (gain 1,000, bandwidth 100-1,000 Hz) and a nerve-cuff stimulation unit. The rat had free access to water and food, except that during H-reflex conditioning it received food mainly by performing the task described below. Animal well-being was carefully checked several times each day, and body weight was measured weekly. Laboratory lights were dimmed from 2100 to 0600 daily.

Stimulus delivery and data collection were under the control of a computer, which monitored soleus EMG activity (sampled at 5,000 Hz) continuously throughout data collection. The soleus H-reflex was elicited as follows. Whenever the absolute value of background (i.e., ongoing) soleus EMG activity remained within a predefined range
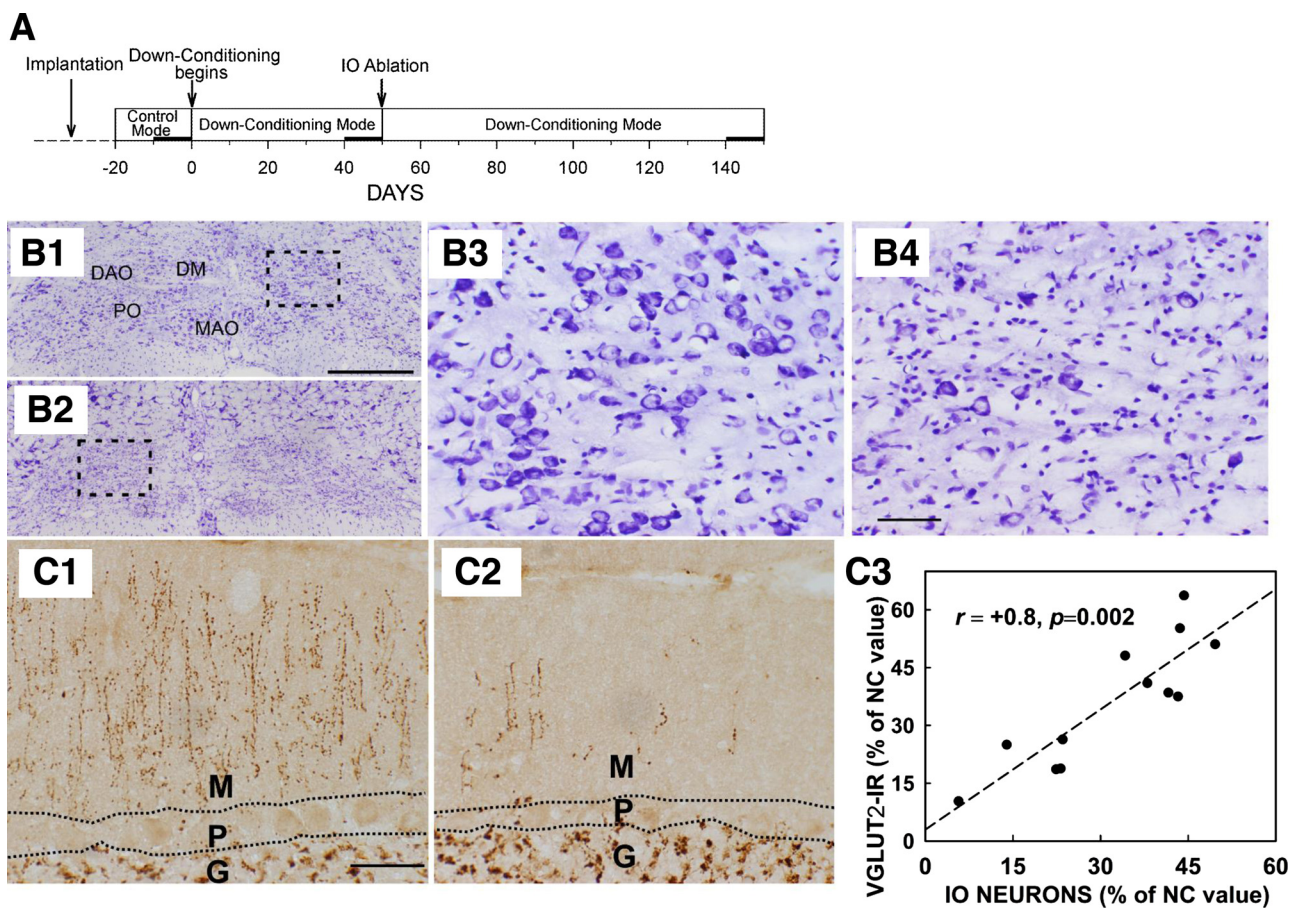

Fig. 1. *A*: Research design. At least 20 days after implantation surgery, rats were exposed to the control mode for 20 days and then to the H-reflex down-conditioning mode for 50 days. The inferior olive (IO) was then ablated. After the ablation, exposure to the down-conditioning mode continued for 56–102 more days. The last 10 control-mode days, the 10 down-conditioning days just before IO ablation (i.e., *days 41–50* of conditioning), and the last 10 days of continued down-conditioning after IO ablation (heavy horizontal lines) provided the data used to assess the effect of down-conditioning on the soleus H-reflex and the final impact of IO ablation on the maintenance of soleus H-reflex down-conditioning. *B*: IO ablation. Cresyl-violet stained photomicrographs showing the IO nucleus complex and IO neurons in a naive control (NC) rat (*B1* and *B3*) and in an IO-ablated rat (IO rat; *B2* and *B4*). (*B3* and *B4* show the areas outlined in *B1* and *B2*, respectively.) DAO, dorsal accessory olive; DM, dorsomedial group; MAO, medial accessory olive; PO, principal olive. Scale bars: 400 μm in *B1* and *B2*, 40 μm in *B3* and *B4*. The loss of most IO neurons in the IO-ablated rat is evident. *C*: VGLUT2 immunoreactivity (VGLUT2-IR) in cerebellar cortex. *C1* and *C2*: photomicrographs of VGLUT2-IR-labeled cerebellar sections showing VGLUT2-IR labeling in cerebellar cortex from a NC rat (*C1*) and an IO rat (*C2*). The molecular (M), Purkinje (P), and granular (G) layers are indicated. VGLUT2-IR in the molecular layer is much weaker in the IO rat (*C2*). Scale bar: 100 μm. *C3*: correlation in IO rats between cerebellar VGLUT2-IR intensity in the molecular layer and remaining IO neurons (in % of NC neuron number). The strong correlation ($r = 0.80$, $P < 0.01$) is consistent with the fact that VGLUT2-IR labeling in the molecular layer is selective for excitatory olivocerebellar climbing fiber terminals on Purkinje cell dendrites (Fremeau et al. 2001; Kaneko et al. 2002).

[typically 1–2% of maximum M-response (i.e., direct muscle response)] for a randomly varying 2.3- to 2.7-s period, the computer stored the most recent 50 ms of EMG activity (i.e., the background EMG interval), delivered a monophasic stimulus pulse through the nerve cuff, and stored the EMG activity for another 100 ms. In the course of its normal activity, the rat typically provided 2,500–7,000 H-reflexes per day.

Stimulus pulse amplitude and duration were initially set to produce a maximum H-reflex and an M-response that was typically just above threshold. After each trial, pulse amplitude was automatically adjusted to maintain the average absolute value of EMG activity in the M-response interval (typically 2.0–4.5 ms) unchanged throughout data collection. Thus, throughout the entire period of data collection, both the background EMG activity (reflecting soleus motoneuron tone at the time of H-reflex elicitation) and the M-response (reflecting the effective strength of the nerve cuff stimulus) remained stable.

M-response size was defined as the average absolute value of EMG activity in the M-response interval minus the average absolute value of background EMG activity. H-reflex size was defined as the average absolute value of EMG activity in the H-reflex interval (typically 6–10 ms after stimulus) minus the average absolute value of background EMG activity and was expressed in units of average background EMG activity (Chen and Wolpaw 1995).

Under the control mode (first 20 days), the computer simply digitized and stored the absolute value of the peristimulus EMG activity. Under the down-conditioning mode, it also gave a food-pellet reward 200 ms after nerve stimulation if the average absolute value of soleus EMG activity in the H-reflex interval was below a criterion value. The criterion value was set and adjusted as needed each day so that the rat received an adequate amount of food (e.g., ~800 reward pellets/day for a 450-g rat). Each rat's number of trials/day, background EMG activity, and M-response size remained stable throughout data collection.

Figure 1A shows the experimental schedule. At least 20 days after electrode implantation, each of 14 rats was exposed to the control mode for 20 days and then to the down-conditioning mode for 50 days. In 12 of the 14 rats down-conditioning was successful [i.e., the H-reflex for *days 41–50* of down-conditioning was ≤80% of its initial value (Chen et al. 2006b; Chen and Wolpaw 1995)]. In the other two rats the H-reflex remained within 20% of its initial value [i.e., down-conditioning failed (Chen and Wolpaw 1995; Wolpaw et al. 1993)], and they were not studied further. In the 12 rats in which down-conditioning was successful the IO was ablated. After IO ablation, down-conditioning exposure continued for an average of 85 (range 56–102) more days.

IO ablation and postablation animal care and well-being. We used a standard pharmacological ablation method to make a selective lesion of the IO: intraperitoneal (ip) injection of 3-acetylpyridine (3-AP), followed several hours later by ip injection of nicotinamide (e.g., Balaban 1985; Gasbarri et al. 2003; Llinas et al. 1975; O'Hearn and Molliver 1997; Saxon and White 2006; Seoane et al. 2005; Watanabe et al. 1997). The dosage and interinjection parameters we adopted have been shown to confine the lesion almost entirely to the IO (Seoane et al. 2005).

Rats were injected with 3-AP (70 mg/kg ip) followed 3.5 h later by nicotinamide (300 mg/kg ip). In the succeeding days, they were carefully watched and checked 4–6 times/day, 7 days/wk. They showed no signs of pain or distress. In the first 24 h, exploratory behavior was attenuated. In subsequent days, they displayed postural and locomotor abnormalities similar to those seen after cerebellar nuclear ablation (Chen and Wolpaw 2005; Wolpaw and Chen 2006) (e.g., splaying of the back limbs, holding the trunk close to the ground, limb rigidity, intermittent hopping locomotion, occasional oscillatory head movements). These overt abnormalities disappeared within 14 days. Rats that ate poorly in the first few days were fed manually with water-soaked rat chow and a high-calorie dietary supplement (Nutri-Cal) until they resumed normal eating (i.e., within 5–10 days). Body

weight, which decreased ~10% in the first week, recovered to its preablation level by 2–3 wk; every rat gained weight over the time of study. Furthermore, after the first 2–3 postablation weeks, rats appeared to walk normally, and they satisfied the background EMG requirement for H-reflex elicitation with the same daily frequency as before ablation, implying that there was no reduction in daily activity level. In light of previous reports (e.g., Denk et al. 1968; Seoane et al. 2005) we suspect that subtle locomotor deficits remained, but they were not readily apparent.

Histology. At the end of data collection, each rat received an overdose of sodium pentobarbital (ip) and was perfused intracardially with 4% paraformaldehyde in 0.1 M phosphate buffer (pH 7.3). The implanted electrodes and tibial nerve were examined, and the right and left soleus muscles were weighed. Five unimplanted naive control (NC) rats with comparable body weights were similarly perfused and processed to provide control histological data.

The brain was removed and postfixed in the same fixative overnight. The area encompassing the IO and the cerebellum was blocked and washed with 0.05 M phosphate-buffered saline (PBS, pH 7.4), infiltrated with 30% sucrose for 24 h, embedded in OCT compound (Tissue-Tek), and frozen with dry ice. Transverse serial sections of IO and cerebellum were cut at 20 μm and 12 μm, respectively, and mounted on precoated glass slides (Superfrost; Fisher). Every fourth IO section was stained with cresyl violet, and every fifth cresyl violet-stained section was photographed with an Olympus BH2-RFCA microscope and an Olympus DF70 digital camera. In each rat, four sections from rostral to caudal [i.e., Ruigrok's level (L)20, L16, L13, and L9 (Ruigrok 2004; Ruigrok and Voogd 2000)] were used for quantitative analysis of the IO ablation (see Chen et al. 2016 for detail). In these sections, we counted on both right and left sides the number of IO cells with diameters of at least 10 μm and obvious Nissl staining around the nucleus (i.e., putative IO neurons) (e.g., Fig. 1, *B3* and *B4*) in a blinded fashion (i.e., whether a given slide came from an normal rat or an IO-ablated rat was unknown to the evaluator). For each IO-ablated rat, the percentage of the IO remaining in each section was defined as [(number of IO neurons in the section)/ (average number of IO neurons in the corresponding section for the 5 NC rats)] × 100.

To determine the impact of IO ablation on olivocerebellar projection fibers, cerebellar vesicular glutamate transporter 2 immunoreactivity (VGLUT2-IR) was assessed with a standard avidin-biotin complex-peroxidase system (ABC Elite; Vector Laboratories, Burlingame, CA) (Chen et al. 2016). Every tenth cerebellar section was processed. The sections were washed with PBS containing 0.1% Triton X-100 (PBST, pH 7.4) three times (10 min each), blocked with 7% normal goat serum for 90 min, and incubated overnight with monoclonal anti-VGLUT2 antibody [Millipore, 1:1,500 dilution in PBST containing 2% bovine serum albumin (BSA)] in a humid chamber at 4°C. They were then washed again and incubated with biotinylated goat anti-mouse secondary antibody (1:200 in PBS) for 1.5 h. Endogenous peroxidase activity was quenched by 0.3% H_2O_2, and then the sections were reacted with the avidin-biotin complex (1:100 in PBS) for 1.5 h. Finally, the sections were reacted with 0.05% diaminobenzidine (DAB) solution containing 0.006% H_2O_2 for 14 min for color development.

VGLUT2-IR is a selective marker for climbing fibers and their terminals in the molecular layer of cerebellar cortex (Fremeau et al. 2001; Kaneko et al. 2002). For each rat, we quantified VGLUT2-IR in the molecular layer by analyzing every fourth VGLUT2-labeled section. Ten photomicrographs were taken from each section with an Olympus BX61 microscope and a Hamamatsu CCD digital camera (×100 magnification, fixed illumination). To sample the entire cerebellar cortex, these photomicrographs were distributed randomly across its entire lateral-to-medial dimension (e.g., Fig. 1H in Chen et al. 2016). In each photomicrograph, the density of VGLUT2-IR terminals was traced with the ImageJ program (version 1.48v) (e.g., Fig. 1, *C1* and *C2*) in a blinded fashion (i.e., whether a given slide

came from a normal rat or an IO-ablated rat was unknown to the evaluator). For each IO rat, cerebellar VGLUT2-IR was calculated in percentage of normal as [(average VGLUT2-IR density of the IO rat)/(average VGLUT2-IR density for the five NC rats)] × 100 (Chen et al. 2016).

While previous studies have shown that the IO ablation regimen does not significantly damage many other brain areas (Gasbarri et al. 2003; Llinas et al. 1975; O'Hearn and Molliver 1997; Saxon and White 2006; Seoane et al. 2005; Watanabe et al. 1997), its potential effects on the spinal cord have not been examined. Thus, to evaluate the possible impact of the IO ablation regimen on spinal cord motoneurons, we assessed the size and number of soleus motoneurons from four randomly selected IO rats and four weight-matched NC rats. Briefly, each rat was perfused as described above. The spinal cord was removed and postfixed. The L_3–L_6 lumbar spinal cord was blocked and washed with 0.05 M PBS (pH 7.4) and infiltrated with 30% sucrose for 24 h, then embedded in OCT compound (Tissue-Tek), and frozen with dry ice. Transverse 25-μm serial sections were cut and mounted onto precoated glass slides (Superfrost; Fisher). Every seventh section was stained with cresyl violet, and every third of these sections was then photographed with an Olympus BH2-RFCA microscope equipped with an Olympus DF70 digital camera. Motoneurons in lamina IX with a diameter of at least 30 μm were counted and measured with the ImageJ program by two independent blinded raters (Wang et al. 2006). Figure 2, *top*, shows representative low (Fig. 2, *top left*)- and high (Fig. 2, *top right*)-magnification photomicrographs of labeled motoneurons from an IO rat and an NC rat. Figure 2, *bottom*, shows the average ($\pm$SE) number of motoneurons/section in L_3, L_4, L_5, and L_6 spinal cord (Fig. 2, *bottom left*) and average ($\pm$SE) L_3–L_6 motoneuron area (Fig. 2, *bottom right*) in IO rats and NC rats. The average numbers of motoneurons in L_3, L_4, L_5, and L_6 spinal cord and the average L_3–L_6 motoneuron area in the IO rats did not differ from those in the NC rats ($P > 0.15$ by t-test). These results support

the conclusion that the IO ablation regimen did not damage lumbar spinal motoneurons.

Data analysis. To assess the effects of IO ablation on the maintenance of H-reflex down-conditioning, a repeated-measures ANOVA was used to compare the average H-reflex size for each 10-day period after IO ablation to the average H-reflex size for the last 10 control-mode days. [For the first 10-day period after IO ablation, the average for *days 3–10* after ablation was used to exclude the transient nonspecific increase in *days 1–2* (Wolpaw and Chen 2006).[1]] If an effect was found, Dunnett's multiple comparisons method was used to identify those 10-day periods that differed significantly from the average of the last 10 control-mode days. In addition, to compare the effects of different lesions [i.e., IO ablation, DIN ablation (Wolpaw and Chen 2006), CST transection (Chen and Wolpaw 2002)] on maintenance of H-reflex down-conditioning, a one-way ANOVA followed by an all-pairwise multiple comparison procedure (Tukey test) was used to compare their final H-reflex sizes.

RESULTS

IO ablation and its impact on climbing fibers. IO ablation was effective. In the IO-ablated rats (IO rats), IO cell counts (i.e., % of the IO remaining) averaged 36($\pm$17 SD)% (range

---

[1] A similar brief increase in H-reflex size also occurred in the first 1-2 days after cerebellar ablation in cats (McLeod and Van Der Meulen 1967; Van Der Meulen and Gilman 1965), DIN ablation in naive or conditioned rats (Chen and Wolpaw 2005; Wolpaw and Chen 2006), or midthoracic transection of the CST, the dorsal column, the dorsal ascending tract, or the lateral column in naive or conditioned rats (Chen et al. 2001a, 2001b, 2003; Chen and Wolpaw 1997, 2002). It is probably a nonspecific short-term effect of the intervention (i.e., surgery or 3-AP injection) and/or (in the case of surgery) the accompanying general anesthesia.
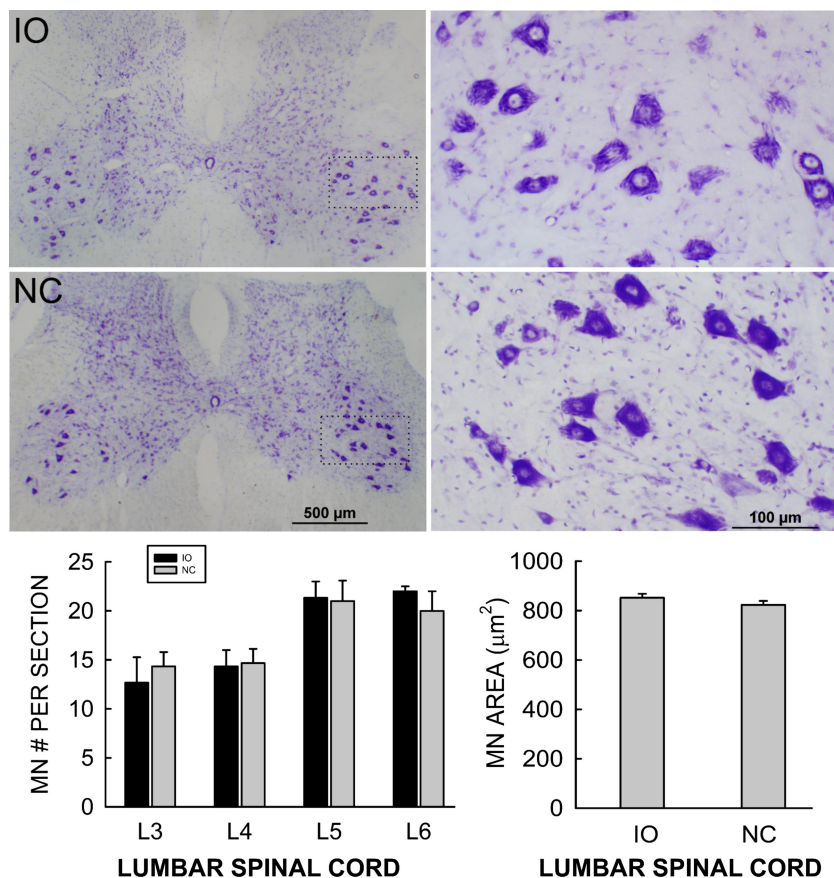

Fig. 2. *Top*: Representative low (*left*)- and high (*right*)-magnification transverse sections of L_5 spinal cord showing labeled motoneurons from an IO rat and an NC rat. *Bottom*: average numbers of motoneurons per section in L_3, L_4, L_5, and L_6 spinal cord (*left*) and average L_3–L_6 motoneuron area (*right*) in IO rats and NC rats ($\pm$SE). Motoneuron number and size did not differ between IO and NC rats ($P > 0.15$ by t-test).

26–46%) of those in NC rats ($P < 0.0001$ for IO vs. normal by t-test). Figure 1B illustrates the IO ablation with sections from a normal rat (Fig. 1, B1 and B3) and an IO rat (Fig. 1, B2 and B4). As noted in previous studies with this 3-AP lesion method (e.g., Seoane et al. 2005) [including our recent study of the impact of IO ablation on the acquisition of H-reflex down-conditioning (Chen et al. 2016)], IO cell loss was greater rostrally than caudally. Chen et al. (2016) provides areal analysis that documents this difference.

As Fig. 1C illustrates, the marked loss of IO neurons was associated with a comparable loss in climbing fiber inputs to the cerebellum. IO ablation produced widespread degeneration of VGLUT2-IR terminals in the molecular layer of cerebellar cortex. [VGLUT2-IR is a selective marker for climbing fibers and their terminals in this layer of cerebellar cortex (Fremeau et al. 2001; Kaneko et al. 2002).] VGLUT2-IR in the molecular layer of IO rats averaged 38($\pm$19 SD)% (range 28–48%) of that in normal rats ($P < 0.0001$ IO vs. normal), and the VGLUT2-IR decrease in IO rats correlated with the decrease in IO cell counts ($r = 0.8$, $P = 0.002$) (i.e., Fig. 1C3). These

results closely paralleled those reported in additional detail in Chen et al. (2016).

Effects of IO ablation on maintenance of a down-conditioned H-reflex. In the 12 rats in which down-conditioning was successful [i.e., the final H-reflex size was ≤80% of the initial value (Chen et al. 2006b; Chen and Wolpaw 1995)], the H-reflex decreased over the 50 days of down-conditioning, reaching 62($\pm$2 SE)% of its initial value for *days 41–50* just prior to IO ablation ($P < 0.001$ vs. initial by paired t-test). Figure 3A shows the average course of this H-reflex decrease and the subsequent changes after IO ablation. After the brief nonspecific rise to 82($\pm$11)% in the first postablation day (see *footnote 1*), H-reflex size fell back to near its preablation value, averaging 59($\pm$6)% for *days 52–60*. It then rose ~15% and remained stable for 30 days, averaging 76($\pm$7)% for *days 61–90*. Beginning at *day 90*, it rose rapidly over 10 days, reaching ~115%, where it remained for 20–25 days before rising further to ~145% for *days 121–140*.

Statistical analysis of the entire course of H-reflex size after the beginning of down-conditioning confirmed this description. A repeated-measures ANOVA applied to the average H-reflex
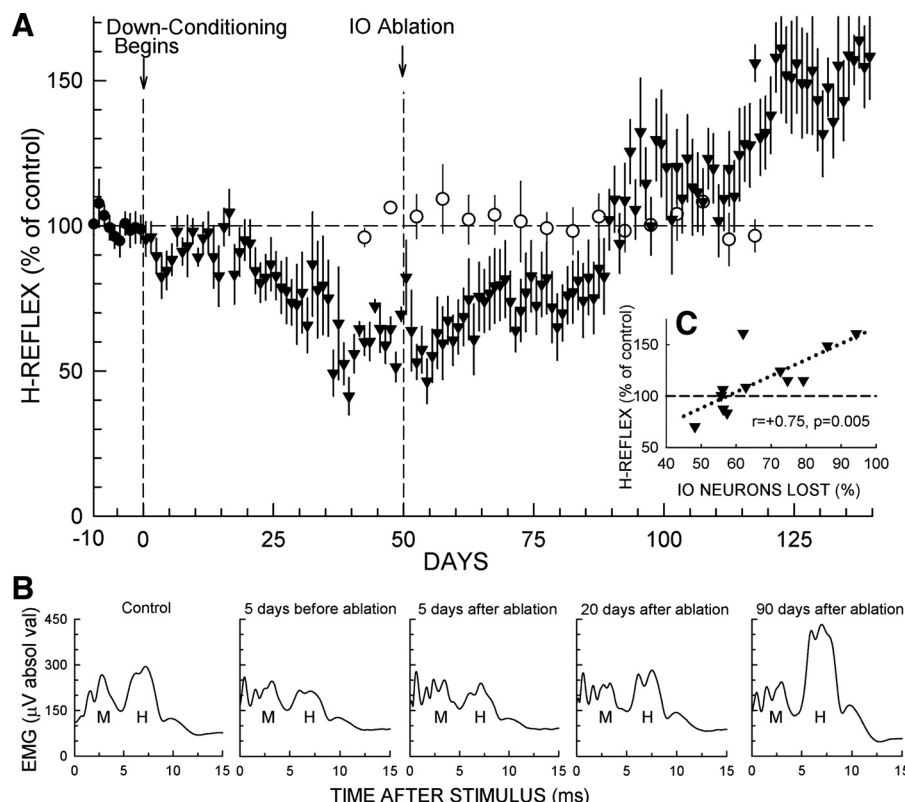

Fig. 3. Effects of IO ablation on H-reflex size in down-conditioned rats and in unconditioned rats. *A*: ▼: average daily H-reflex ($\pm$SE) (in % of initial size) for the 12 IO rats for the final 10 days in control mode and for up to 140 days of exposure to the down-conditioning mode. As shown, the IO was ablated after the first 50 days of down-conditioning. All 12 rats were then studied through *day 106* (56 days after ablation); 11 were studied through *day 112*; and 7 were studied through *day 140* (90 days after ablation). H-reflex size averaged 62($\pm$2)% of initial value for the 10 days immediately before IO ablation ($P < 0.001$). It rose to ~75% in the next 10 days, remained there for ~30 days, and then over the next 10 days rose to above its initial value and remained high [140($\pm$14)% for each rat's final 10 days of data collection ($P = 0.005$ vs. initial)]. Background EMG amplitude and M-response size were stable throughout. ○: 5-day average H-reflex ($\pm$SE) size (in % of initial size) for 7 rats exposed to the control-mode before and for 50–70 days after IO ablation. All 7 rats were followed for 50 days after ablation, and 5 were followed for 70 days. Background EMG amplitude and M-response size were stable throughout. In these unconditioned rats, IO ablation had no detectable long-term effect on H-reflex size [data from Chen et al. (2016) plus additional more recent data]. *B*: average daily poststimulus EMG activity from a representative IO rat for: a control-mode day; 5 days prior to IO ablation; 5 days after IO ablation; 20 days after IO ablation; and 90 days after IO ablation. The early and delayed increases following IO ablation are evident. Background EMG amplitude (i.e., the amplitude at *time 0*) and M-response size are stable throughout. *C*: average H-reflex size for *days 101–110* (51–60 days after IO ablation) for each IO rat vs. the percent of IO ablated [i.e., 100 − (no. of IO neurons remaining in % of average number in NC rats)]. H-reflex size is strongly correlated with IO neuronal loss, implying that the IO plays a key role in the preservation of the H-reflex decrease produced by down-conditioning.

values of the 10-day periods from *days 1–10* through *days 131–140* showed significant variation from the average of the last 10 control-mode days ($P < 0.001$). Dunnett's multiple comparisons test indicated that the average H-reflexes for *days 31–40* through *days 71–80* were significantly smaller than the average control H-reflexes ($P < 0.01$ for each period from *days 31–40* through *days 61–70*, $P < 0.05$ for *days 71–80*) and that the average H-reflexes for *days 121–130* and *days 131–140* were significantly larger than the average control H-reflexes ($P < 0.01$ for each period).

Figure 3*B* shows average daily H-reflexes from one IO rat: in the control-mode period before down-conditioning; 5 days before IO ablation; 5 days after IO ablation; 20 days after IO ablation; and 90 days after IO ablation. These illustrate the decrease produced by down-conditioning, the loss of some of the decrease by 2 wk after ablation, and the delayed large increase that produces a final H-reflex greater than control. To evaluate the relationship between the severity of the IO ablation and the impairment of down-conditioning maintenance, we determined the correlation between the percentage of IO neurons lost and the H-reflex size for *days 101–110* (i.e., 51–60 days after ablation, and the last 10-day period for which all 12 rats had data). As Fig. 3*C* shows, H-reflex size was strongly correlated with IO neuronal loss (i.e., $r = 0.75$, $P < 0.01$). (Comparable correlations were present for the subsequent 10-day periods.) This finding implies that greater IO damage produced greater loss of down-conditioning.

For comparison with the data from down-conditioned rats, Fig. 3*A* also includes recent data (Chen et al. 2016 plus additional unpublished data) showing the impact of IO ablation on H-reflex size in naive unconditioned rats. It is clear that IO ablation has no long-term impact on the H-reflex in unconditioned rats; the multistage postablation increase in H-reflex size occurs only in the down-conditioned rats.

DISCUSSION

IO ablation and its possible effects on the H-reflex. As summarized and illustrated in RESULTS and described in detail previously (Chen et al. 2016), the regimen of 3-AP injection followed by nicotinamide destroyed most of the IO, and this loss correlated with loss of climbing fiber inputs to cerebellum. Past studies have established the IO specificity of this ablation regimen [particularly with the dosage and timing parameters used in the present study (Seoane et al. 2005)]. Our finding that this ablation regimen does not affect spinal lumbar motoneuron number or size (Fig. 2) provides further support for its specificity. Earlier studies have also shown that the IO lesion develops quickly, in the first 24 h after AP injection (Balaban 1985; Gasbarri et al. 2003; Llinas et al. 1975; O'Hearn and Molliver 1997; Saxon and White 2006; Seoane et al. 2005; Watanabe et al. 1997). Taken together, the results of past studies and our spinal cord histology indicate that the acceptance and interpretation of the present H-reflex data should not be significantly compromised by concerns about the severity, specificity, or rapidity of the IO ablation.

IO lesions are followed by histological and functional effects that develop gradually and appear to reflect recovery processes or other long-term changes (Aoki and Sugihara 2012; Bardin et al. 1983; Benedetti et al. 1984; Lutes et al. 1992; Rossi et al. 1991a, 1991b). However, in naive (i.e., unconditioned) rats IO

ablation alone [like DIN ablation alone (Chen and Wolpaw 2005)] has no detectable long-term effect on H-reflex size (Chen et al. 2016). As Fig. 3*A* shows, the striking long-term postablation H-reflex changes reported here occur only in rats that were down-conditioned prior to IO ablation. Furthermore, given that the rats of this study continued under the down-conditioning mode through the postablation period, the sequential increases in H-reflex size represent delayed losses of function rather than recovery of function. In sum, the long-term H-reflex increases that occur in down-conditioned rats are not due simply to the IO ablation alone; rather they appear to reflect the delayed deleterious impact of IO ablation on the maintenance of a decreased H-reflex.

Lesion effects on maintenance of a down-conditioned H-reflex. Transection of the dorsal ascending tract or the ipsilateral lateral column does not impair maintenance of a down-conditioned H-reflex, while CST transection or DIN ablation does do so (Chen and Wolpaw 1997, 2002). Figure 4*A* compares the effects of IO ablation on maintenance of down-conditioning found in the present study with the effects of DIN ablation or CST transection (Chen and Wolpaw 1997, 2002, 2005; Wolpaw and Chen 2006). All three lesions show the transient nonspecific increase in the first 1–2 postlesion days (see *footnote 1*). Then, 5–10 days after CST transection or 40–50 days after DIN or IO ablation, the H-reflex rises to significantly above its original control size, despite continued exposure to the down-conditioning mode (Chen and Wolpaw 2002; Wolpaw and Chen 2006). This high value remains through the end of data collection.

Statistical analysis confirmed this description. One-way ANOVA indicated that the final H-reflex values (i.e., average H-reflex size for the final 10 days of data collection after IO or DIN ablation or CST transection) did not differ for the three different lesions ($P = 0.73$). CST transection, DIN ablation, and IO ablation had similar final effects: an H-reflex significantly larger than control [$125(\pm 8$ SE)%, $130(\pm 9)$%, and $140(\pm 14)$% for CST, DIN, and IO rats, respectively, for the final 10 days of data collection]. The notable difference was that after CST transection this high value was reached within 10 days, while after DIN or IO ablation the H-reflex increased in two stages and the high value was not reached until 50 days after the lesion.

While the course of change in H-reflex size after IO ablation was similar to that after DIN ablation, it differed in one respect. Figure 4*B* shows the average daily H-reflex values for the days immediately before and after IO or DIN ablation. After DIN ablation, the first stage of postablation H-reflex increase occurred within 2 days. H-reflex sizes for the 10 days before and *days 3–10* after DIN ablation averaged $56(\pm 5$ SE)% and $74(\pm 5)$%, respectively. This marked increase was significant ($P = 0.007$ by paired t-test). In contrast, after IO ablation, the first stage of postablation H-reflex increase developed over ~10 days. H-reflex sizes for the 10 days before and *days 3–10* after IO ablation averaged $62(\pm 2)$% and $58(\pm 6)$%, respectively, and did not differ significantly ($P = 0.4$). [*Days 1* and *2* after ablation were omitted from these pre/postablation comparisons because of the transient nonspecific postlesion increase (i.e., *footnote 1*).] The difference between the two ablations in the timing of the first stage of postablation H-reflex increase has important implications (see below).
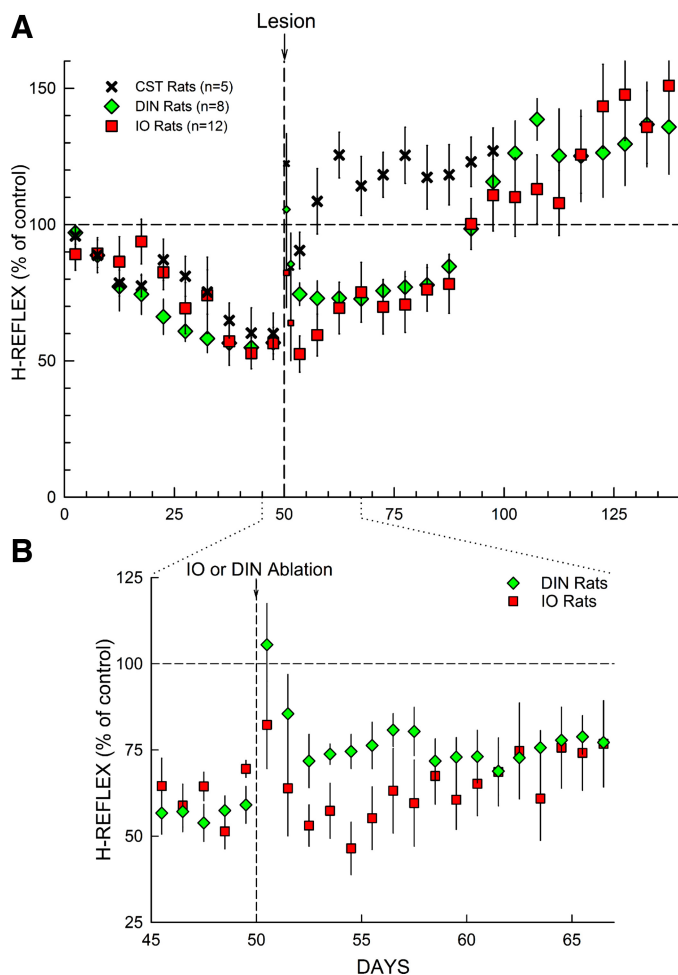
Fig. 4. *A*: effects of different lesions on maintenance of H-reflex down-conditioning. Average H-reflex sizes (±SE) for each 5-day period for corticospinal tract (CST)-transected rats (*n* = 5), DIN-ablated rats (*n* = 8), and IO-ablated rats (*n* = 12) for the first 50 days of down-conditioning before the lesion and for the next 50–100 days after the lesion [CST data from Chen and Wolpaw (2002); DIN data from Wolpaw and Chen (2006); IO data from present study]. For the 5 days immediately after lesion, H-reflex sizes are shown for the 1st day and the 2nd day (smaller symbols) and for the next 3 days together. All 3 lesions show a transient increase in the first 1–2 days (see *footnote 1*). After this brief nonspecific effect dissipates, all 3 lesions result eventually in an H-reflex larger than its initial control size. The H-reflex down-conditioning mode remains in effect throughout. *B*: this expansion from *A* shows average daily H-reflex values for the IO and DIN rats for the days immediately before and after IO or DIN ablation. In the DIN rats, the first stage of the H-reflex increase occurs within the first 2 days after DIN ablation; in the IO rats, it develops over the initial 10 days after IO ablation. [The brief nonspecific increase in the first 1–2 postablation days is evident for both ablations (*footnote 1*).]

IO ablation vs. DIN ablation. Like DIN ablation, IO ablation has no long-term impact on H-reflex size in naive (i.e., unconditioned) rats (Fig. 3*A*), and it entirely prevents acquisition of a down-conditioned H-reflex (Chen et al. 2016). The present results show that, like DIN ablation (Wolpaw and Chen 2006), IO ablation after down-conditioning leads to a two-stage loss of the H-reflex decrease and a final H-reflex that is significantly larger than its initial value. The difference between the effects of the two ablations is that the first stage of the loss occurs immediately (i.e., in the first 1–2 days) after DIN ablation, while after IO ablation it develops over ~10 days.

The IO and DIN ablation results raise three questions. First, do their similarities confirm and extend the conclusions drawn previously from the DIN results about the role of the cerebellum in H-reflex down-conditioning (Chen and Wolpaw 2005; Wolpaw and Chen 2006)? Second, what insight does the difference between the effects of DIN and IO ablations provide about the role of the IO? Third, what can now be said about how a down-conditioned H-reflex is acquired and maintained?

Role of the cerebellum in H-reflex down-conditioning. Both acquisition and long-term maintenance of H-reflex down-conditioning are prevented by DIN ablation or CST transection and are not prevented by transection of other major descending pathways, including the rubrospinal, reticulospinal, and vestibulospinal tracts (Chen and Wolpaw 1997, 2002, 2005; Wolpaw and Chen 2006). Thus it appears that the essential cerebellar contribution is output that goes to sensorimotor cortex (SMC; the principal origin of the CST) rather than to the spinal cord. This cerebellocortical input might guide the CST activity that produces the spinal cord plasticity that is directly responsible for the smaller H-reflex. Alternatively, it might simply be needed for the normal functioning of SMC that enables it to produce the crucial CST activity.

The present finding that IO ablation prevents the long-term maintenance of down-conditioning as effectively as DIN ablation supports the hypothesis that the IO and the cerebellum guide the CST activity that changes the H-reflex. A nonspecific global effect of IO ablation on SMC function is less likely because IO ablation (like DIN ablation) had no lasting effect on animal well-being, gross motor behavior, or activity level (see METHODS). Furthermore, IO output is more distantly connected to SMC than cerebellar output, and the total loss of down-conditioning after IO ablation occurs only after a long delay. These findings suggest that the impact of IO ablation on down-conditioning is not due to a nonspecific impairment of cortical function. Furthermore, the distinct difference in the effects of IO and DIN ablations on the maintenance of down-conditioning suggests that cerebellar plasticity has a key role in H-reflex down-conditioning, and that this plasticity is guided and maintained by the IO.

Role of the IO in H-reflex down-conditioning. After DIN or IO ablation, the loss of the H-reflex decrease occurs in two stages, an initial increase of ~15% followed much later by a greater increase that results in an H-reflex larger than its original size. Similar increases have been noted under other circumstances in both monkeys and rats (Chen et al. 2006a; Chen and Wolpaw 2002; Wolpaw and Chen 2006; Wolpaw and Lee 1989). Their origins are considered in Wolpaw and Chen (2006). They are consistent with the abundant evidence that H-reflex conditioning entails plasticity at multiple sites in the spinal cord and brain (see for review Thompson and Wolpaw 2014; Wolpaw 2010; Wolpaw and Chen 2009;). Considered in terms of the new skill, a modified H-reflex, these changes at multiple sites fall into three categories. "Primary plasticity" comprises the changes responsible for the H-reflex increase or decrease that was the goal of the conditioning protocol; "compensatory plasticity" comprises the changes that preserve older skills that were disturbed by the primary plasticity; and "reactive plasticity" comprises the changes caused by altered activity due to primary or compensatory plasticity (Chen et al. 2011; Wolpaw 1997, 2010; Wolpaw and Lee 1989; Wolpaw and Tennissen 2001). In the present context of H-re-

flex down-conditioning, the initial postablation increase is not adaptive; it detracts from the conditioned decrease in the H-reflex and thereby makes reward less likely. Thus it is likely to reflect either compensatory or reactive plasticity that is revealed by the ablation.

In rats that are down-conditioned prior to DIN or IO ablation, the initial increase appears immediately or soon after the ablation, respectively. It then coexists with the large H-reflex decrease produced by down-conditioning until that decrease disappears 40–50 days after the ablation. From then on, the initial increase is evident as an increase above the original H-reflex size. The fact that the initial increase appears immediately after DIN ablation implies that cerebellar output was suppressing it previously (Wolpaw and Chen 2006). The present finding that the increase occurred over ~10 days after IO ablation suggests that its suppression depended on cerebellar cortical (and/or nuclear) plasticity that was being maintained by IO input.

Two other models of motor learning, vestibuloocular reflex conditioning and eyeblink conditioning, are thought to involve cerebellar plasticity caused by the conjunction of activity in specific mossy and climbing fibers (Boyden et al. 2004; Cheron et al. 2013; Freeman and Steinmetz 2011; Ito 1982; Longley and Yeo 2014; Mauk et al. 2014; Schonewille et al. 2011; Thompson 2005; Welsh et al. 2005). The climbing fibers, which originate in the IO, are hypothesized to provide a teaching signal.

A comparable conjunction could underlie H-reflex conditioning. The mossy fibers might convey efference-copy activity reflecting current CST influence over the H-reflex pathway (Leergaard et al. 2006; Ruigrok et al. 2015; Suzuki et al. 2012). The climbing fibers might indicate whether a reward occurs (e.g., whether the IO receives input caused by the click of the pellet dispenser or the consumption of the food pellet) (see Ruigrok et al. 2015 for review of IO inputs). The cerebellar output to SMC resulting from this conjunction could increase the probability of CST activity that decreases the H-reflex, and thus increases the probability of reward. By providing evidence for cerebellar plasticity, the difference between DIN ablation and IO ablation in the rate of the initial postablation H-reflex increase supports this possibility.

In addition to their role in suppressing the H-reflex increase, the IO and cerebellum appear to be essential for creation and long-term survival of the H-reflex decrease that is the goal of down-conditioning. This is the decrease that disappears 40–50 days after IO or DIN ablation. The long delay implies that the decrease reflects SMC (or closely related) plasticity that produces the essential CST activity and can survive for ~6 wk after DIN or IO ablation abolishes the cerebellar influence that induces and maintains it. The evidence that cerebellar plasticity suppresses the H-reflex increase (i.e., Fig. 4B) suggests that cerebellar plasticity is also responsible for induction and maintenance of the SMC plasticity underlying the H-reflex decrease. If this is correct, the delay prior to loss of the H-reflex decrease should be 5–10 days longer after IO ablation than after DIN ablation (i.e., because the loss of the crucial cerebellar input to SMC, which occurs immediately after DIN ablation, should not occur until 5–10 days after IO ablation when the cerebellar plasticity that had been maintained by the IO disappears). The present data (i.e., *days 90–140* in Fig. 4A) do suggest that the loss takes longer after IO ablation; however, more data are needed to

settle this issue. Finally, the key role of the IO in down-conditioning is further indicated by the strong positive correlation between IO neuronal loss and loss of a smaller H-reflex (Fig. 3C). Confirmation of the hypothesis that mossy and climbing fiber inputs combine to produce cerebellar plasticity that underlies H-reflex down-conditioning will entail characterization of these inputs, description of the resulting plasticity, and demonstration that the inputs and the plasticity are necessary and sufficient for reducing the H-reflex.

Multisite plasticity underlying H-reflex down-conditioning. The plasticity directly responsible for the smaller H-reflex is largely in the spinal cord. It is thought to include a positive shift in motoneuron firing threshold that may reflect a change in sodium channels in the motoneuron membrane produced by metabotropic input to the motoneuron from GABAergic interneurons in the ventral horn that receive the essential CST input (Carp et al. 2001; Carp and Wolpaw 1994; Halter et al. 1995; Pillai et al. 2008; Wang et al. 2006, 2009). The impact of CST transection on a down-conditioned H-reflex implies that this spinal cord plasticity survives only 5–10 days without the CST input (Chen and Wolpaw 1997, 2002). The delayed
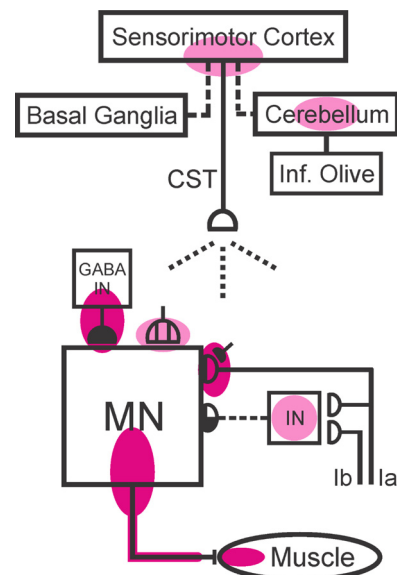

Fig. 5. Present knowledge of the multisite brain and spinal cord plasticity underlying H-reflex conditioning. Shaded ovals indicate the spinal and supraspinal sites of definite or probable plasticity associated with operant conditioning of the spinal stretch reflex (SSR) or its electrical analog, the H-reflex. MN, the motoneuron; CST, the main corticospinal tract; IN, a spinal interneuron; GABA IN, a GABAergic spinal interneuron. Open synaptic terminals are excitatory, solid ones are inhibitory, half-open ones could be either, and the subdivided one is a cluster of C terminals. Dashed pathways imply the possibility of intervening spinal interneurons. The monosynaptic and probably oligosynaptic SSR/H-reflex pathway from Ia and Ib afferents to the motoneuron is shown. Definite (red shading) or probable (pink shading) sites of plasticity include: the motoneuron membrane (i.e., firing threshold and axonal conduction velocity); motor unit properties; GABAergic interneurons in the ventral horn; GABAergic inhibitory terminals, C terminals, and Ia afferent terminals on the motoneuron; terminals conveying disynaptic group I inhibition or excitation to the motoneuron; sensorimotor cortex (SMC); and cerebellum. The essential roles of the corticospinal tract (which originates largely in SMC), cerebellar and basal ganglia output to cortex, and inferior olive input to cerebellum are indicated. The spinal cord plasticity that is directly responsible for H-reflex conditioning appears to be induced and maintained by cortical plasticity that may depend for its long-term survival on cerebellar plasticity that in turn depends for its survival on input from the inferior olive (see text). [Updated from Wolpaw (2010) with permission.]

impact of DIN or IO ablation implies that the CST input depends on SMC (or closely related) plasticity that survives 40–50 days without cerebellar influence.

Cerebellar-cerebral interactions help to guide the activity-dependent SMC plasticity underlying the acquisition of new behaviors. For example, the cerebellum is likely to play a key role in intrinsic rehearsal of new learning and in regulating adaptive changes in cortical excitability (Andre and Arrogi 2003; Garrido et al. 2013; Houk 1997; Luft et al. 2005; Middleton and Strick 1998; Molinari et al. 2002; Schmahmann and Pandyat 1997). The impact of IO ablation described in the present study implies that the SMC plasticity responsible for the critical CST output depends on the IO and the cerebellum for its long-term survival, and it suggests that part (at least) of the total H-reflex decrease (i.e., the decrease present before CST, DIN, or IO ablation) depends on cerebellar plasticity that survives only ~10 days without the IO.

In down-conditioned rats, CST transection, DIN ablation, and IO ablation all lead to the same final result: an H-reflex larger than its initial value (i.e., Fig. 4*A*). The different time courses by which each lesion produces this final result suggest that H-reflex down-conditioning depends on a hierarchy of brain and spinal cord plasticity. This hierarchy may begin with the conjunction in the cerebellum of a reward signal from the IO with a copy of the CST activity that influences H-reflex size. The conjunction may establish plasticity in cerebellum and SMC that establishes and maintains the spinal cord plasticity that is directly responsible for the smaller H-reflex. The final postlesion increase above the initial H-reflex size suggests additional spinal or supraspinal plasticity that serves to preserve previously acquired behaviors (i.e., compensatory plasticity) (Chen et al. 2011; Wolpaw 2010; Wolpaw and Lee 1989; Wolpaw and Tennissen 2001). When the hierarchy is intact, the effect of this additional plasticity on the H-reflex is not apparent. It becomes apparent only when the hierarchy is disrupted [e.g., by IO ablation (present study), DIN ablation (Wolpaw and Chen 2006), CST transection (Chen and Wolpaw 2002), or complete spinal cord transection (Wolpaw and Lee 1989)].

Figure 5 summarizes the sites of definite or probable plasticity in the brain and spinal cord associated with H-reflex conditioning. The present results combine with previous data to suggest that the IO guides H-reflex change by inducing and maintaining cerebellar plasticity that induces and maintains cortical plasticity that induces and maintains CST activity that induces and maintains the spinal cord plasticity that is directly responsible for the smaller H-reflex. Thus they further define the hierarchy of plasticity that appears to underlie this simple learning (Wolpaw and Chen 2006), and they extend it back toward its origin in the reward contingency imposed by the operant conditioning protocol. Comparable hierarchies may underlie other motor learning.

DISCLOSURES

AUTHOR CONTRIBUTIONS

X.Y.C. and J.R.W. conception and design of research; X.Y.C., Y.W., Y.C., and L.C. performed experiments; X.Y.C., Y.W., Y.C., L.C., and J.R.W. analyzed data; X.Y.C., Y.W., Y.C., L.C., and J.R.W. interpreted results of experiments; X.Y.C., Y.W., Y.C., and L.C. prepared figures; X.Y.C., Y.W., Y.C., and J.R.W. drafted manuscript; X.Y.C. and J.R.W. edited and revised manuscript; X.Y.C., Y.W., Y.C., L.C., and J.R.W. approved final version of manuscript.

REFERENCES

Andre P, Arrogi P. Hipnic modulation of cerebellar information processing: implications for the cerebro-cerebellar dialogue. *Cerebellum* 2: 84–95, 2003.

Aoki H, Sugihara I. Morphology of single olivocerebellar axons in the denervation-reinnervation model produced by subtotal lesion of the rat inferior olive. *Brain Res* 1449: 24–37, 2012.

Balaban CD. Central neurotoxic effects of intraperitoneal administered 3-acetylpyridine, harmaline and nicotinamide in Sprague-Dawley and Long-Evans rats: a critical review of 3-acetyl-pyridine neurotoxicity. *Brain Res Rev* 9: 21–42, 1985.

Bardin JM, Batini C, Billard JM, Buisseret-Delmas C, Conrath-Verrier M, Corvaja N. Cerebellar output regulation by the climbing and mossy fibers with and without the inferior olive. *J Comp Neurol* 213: 464–477, 1983.

Benedetti F, Montarolo PG, Rabacchi S. Inferior olive lesion induces long-lasting functional modification in the Purkinje cells. *Exp Brain Res* 55: 368–371, 1984.

Boyden ES, Katoh A, Raymond JL. Cerebellum-dependent learning: the role of multiple plasticity mechanisms. *Annu Rev Neurosci* 27: 581–609, 2004.

Carp JS, Chen XY, Sheikh H, Wolpaw JR. Operant conditioning of rat H-reflexes affects motoneuron axonal conduction velocity. *Exp Brain Res* 136: 269–273, 2001.

Carp JS, Wolpaw JR. Motoneuron plasticity underlying operantly conditioned decrease in primate H-reflex. *J Neurophysiol* 72: 431–442, 1994.

Carrier L, Brustein S, Rossignol S. Locomotion of the hindlimbs after neurectomy of ankle flexors in intact and spinal cats. *J Neurophysiol* 77: 1979–1993, 1997.

Chen XY, Carp JS, Chen L, Wolpaw JR. Corticospinal tract transection prevents operantly conditioned H-reflex increase in rats. *Exp Brain Res* 144: 88–94, 2002.

Chen XY, Carp JS, Chen L, Wolpaw JR. Sensorimotor cortex ablation prevents H-reflex up-conditioning and causes a paradoxical response to down-conditioning in rats. *J Neurophysiol* 96: 119–127, 2006a.

Chen XY, Chen L, Wolpaw JR. Time course of H-reflex conditioning in the rat. *Neurosci Lett* 302: 85–88, 2001a.

Chen XY, Chen L, Wolpaw JR. Conditioned H-reflex increase persists after transection of the main corticospinal tract in rats. *J Neurophysiol* 90: 3572–3578, 2003.

Chen XY, Feng-Chen KC, Chen L, Stark DM, Wolpaw JR. Short-term and medium-term effects of spinal cord tract transections on soleus H-reflex in freely moving rats. *J Neurotrauma* 18: 313–327, 2001b.

Chen XY, Wang Y, Chen Y, Chen L, Wolpaw JR. Ablation of the inferior olive prevents H-reflex down-conditioning in rats. *J Neurophysiol* 115: 1630–1636, 2016.

Chen XY, Wolpaw JR. Operant conditioning of H-reflex in freely moving rats. *J Neurophysiol* 73: 411–415, 1995.

Chen XY, Wolpaw JR. Dorsal column but not lateral column transection prevents down-conditioning of H-reflex in rats. *J Neurophysiol* 78: 1730–1734, 1997.

Chen XY, Wolpaw JR. Probable corticospinal tract control of spinal cord plasticity in rats. *J Neurophysiol* 87: 645–652, 2002.

Chen XY, Wolpaw JR. Ablation of cerebellar nuclei prevents H-reflex down-conditioning in rats. *Learn Mem* 12: 248–254, 2005.

Chen Y, Chen L, Wang Y, Wolpaw JR, Chen XY. Operant conditioning of rat soleus H-reflex oppositely affects another H-reflex and changes locomotor kinematics. *J Neurosci* 31: 11370–11375, 2011.

Chen Y, Chen XY, Jakeman LB, Schalk G, Stokes BT, Wolpaw JR. The interaction of a new motor skill and an old one: H-reflex conditioning and locomotion in rats. *J Neurosci* 25: 6898–6906, 2005.

Chen Y, Chen XY, Jakeman LB, Chen L, Stokes BT, Wolpaw JR. Operant conditioning of H-reflex can correct a locomotor abnormality after spinal cord injury in rats. *J Neurosci* 26: 12537–12543, 2006b.

Cheron G, Dan B, Márquez-Ruiz J. Translational approach to behavioral learning: lessons from cerebellar plasticity. *Neural Plast* 2013: 853654, 2013.

Denk H, Haider MS, Kovac W, Studynka G. Verhaltensanderung und Neuropathologie bei der 3-Acetylpyridinvergiftung der Ratte. *Acta Neuropathologica* 10: 34–44, 1968.

Freeman JH, Steinmetz AB. Neural circuitry and plasticity mechanisms underlying delay eyeblink conditioning. *Learn Mem* 18: 666–677, 2011.

Fremeau RT Jr, Troyer MD, Pahner I, Nygaard GO, Tran CH, Reimer RJ, Bellocchio EE, Fortin D, Storm-Mathisen J, Edwards RH. The expression of vesicular glutamate transporters defines two classes of excitatory synapse. *Neuron* 31: 247–260, 2001.

Garrido JA, Luque NR, D'Angelo E, Ros E. Distributed cerebellar plasticity implements adaptable gain control in a manipulation task: a closed-loop robotic simulation. *Front Neural Circuits* 7: 159, 2013.

Gasbarri A, Pompili A, Pacitti C, Cicirata F. Comparative effects of lesions to the ponto-cerebellar and olive-cerebellar pathways on motor and spatial learning in the rat. *Neuroscience* 116: 1131–1140, 2003.

Halter JA, Carp JS, Wolpaw JR. Operantly conditioned motoneuron plasticity: possible role of sodium channels. *J Neurophysiol* 74: 867–871, 1995.

Houk JC. On the role of the cerebellum and basal ganglia in cognitive signal processing. *Prog Brain Res* 114: 543–552, 1997.

Ito M. Cerebellar control of the vestibulo-ocular reflex—around the flocculus hypothesis. *Annu Rev Neurosci* 5: 275–296, 1982.

Kaneko T, Fujiyama F, Hioki H. Immunohistochemical localization of candidates for vesicular glutamate transporters in the rat brain. *J Comp Neurol* 444: 39–62, 2002.

Leergaard TB, Lillehaug S, Schutter ED, Bower JM, Bjaalie JG. Topographical organization of pathways from somatosensory cortex through the pontine nuclei to tactile regions of the rat cerebellar hemispheres. *Eur J Neurosci* 24: 2801–2812, 2006.

Lieb JR, Frost WN. Realistic simulation of the *Aplysia* siphon-withdrawal reflex circuit: roles of circuit elements in producing motor output. *J Neurophysiol* 77: 1249–1268, 1997.

Llinas R, Walton K, Hillman DE, Sotelo C. Inferior olive: its role in motor learning. *Science* 190: 1230–1231, 1975.

Longley M, Yeo CH. Distribution of neural plasticity in cerebellum-dependent motor learning. *Prog Brain Res* 210: 79–101, 2014.

Luft AR, Manto MU, Ben Taib NO. Modulation of motor cortex excitability by sustained peripheral stimulation: the interaction between the motor cortex and the cerebellum. *Cerebellum* 4: 90–96, 2005.

Lutes J, Lorden JF, Davis BJ, Oltmans GA. GABA levels and GAD immunoreactivity in the deep cerebellar nuclei of rats with altered olivocerebellar function. *Brain Res Bull* 29: 329–336, 1992.

Martin TA, Keating JG, Goodkin HP, Bastian AJ, Thach WT. Throwing while looking through prisms. I. Focal olivocerebellar lesions impair adaptation. *Brain* 119: 1183–1198, 1996.

Mauk MD, Li W, Khilkevich A, Halverson H. Cerebellar mechanisms of learning and plasticity revealed by delay eyelid conditioning. *Int Rev Neurobiol* 117: 21–37, 2014.

McLeod JG, Van Der Meulen JP. Effect of cerebellar ablation on the H reflex in the cat. *Arch Neurol* 16: 421–432, 1967.

Middleton FA, Strick PL. Cerebellar output: motor and cognitive channels. *Trends Cogn Sci* 2: 348–354, 1998.

Molinari M, Filippini V, Leggio MG. Neuronal plasticity of interrelated cerebellar and cortical networks. *Neuroscience* 111: 863–870, 2002.

O'Hearn E, Molliver ME. The olivocerebellar projection mediates ibogaine-induced degeneration of Purkinje cells: a model of indirect, trans-synaptic excitotoxicity. *J Neurosci* 17: 8828–8841, 1997.

Pillai S, Wang Y, Wolpaw JR, Chen XY. Effects of H-reflex up-conditioning on GABAergic terminals on rat soleus motoneurons. *Eur J Neurosci* 28: 668–674, 2008.

Rossi F, van der Want JJ, Wiklund L, Strata P. Reinnervation of cerebellar Purkinje cells by climbing fibres surviving a subtotal lesion of the inferior olive in the adult rat. II. Synaptic organization on reinnervated Purkinje cells. *J Comp Neurol* 308: 536–554, 1991a.

Rossi F, Wiklund L, van der Want JJ, Strata P. Reinnervation of cerebellar Purkinje cells by climbing fibres surviving a subtotal lesion of the inferior olive in the adult rat. I. Development of new collateral branches and terminal plexuses. *J Comp Neurol* 308: 513–535, 1991b.

Ruigrok TJ. Precerebellar nuclei and red nucleus. In: *The Rat Nervous System* (3rd ed.), edited by Paxinos G. San Diego, CA: Elsevier, 2004, p. 180–187.

Ruigrok TJ, Sillitoe RV, Voogd J. Cerebellum and cerebellar connections. In: *The Rat Nervous System* (4th ed.), edited by Paxinos G. San Diego, CA: Elsevier, 2015, p. 133–205.

Ruigrok TJ, Voogd J. Organization of projections from the inferior olive to the cerebellar nuclei in the rat. *J Comp Neurol* 426: 209–228, 2000.

Saxon DW, White G. Episodic vestibular disruption following ablation of the inferior olive in rats: behavioral correlates. *Behav Brain Res* 175: 128–138, 2006.

Schmahmann JD, Pandyat DN. The cerebrocerebellar system. *Int Rev Neurobiol* 41: 31–60, 1997.

Schonewille M, Gao Z, Boele HJ, Vinueza Veloz MF, Amerika WE, Simek AA, De Jeu MT, Steinberg JP, Takamiya K, Hoebeek FE, Linden DJ, Huganir RL, De Zeeuw CI. Reevaluating the role of LTD in cerebellar motor learning. *Neuron* 70: 43–50, 2011.

Seoane A, Apps R, Balbuena E, Herrero L, Llorens J. Differential effects of trans-crotononitrile and 3-acetylpyridine on inferior olive integrity and behavioural performance in the rat. *Eur J Neurosci* 22: 880–894, 2005.

Shmuelof L, Krakauer JW. Are we ready for a natural history of motor learning? *Neuron* 72: 469–476, 2011.

Suzuki L, Coulon P, Sabel-Goedknegt EH, Ruigrok TJ. Organization of cerebral projections to identified cerebellar zones in the posterior cerebellum of the rat. *J Neurosci* 32: 10854–10869, 2012.

Thompson AK, Wolpaw JR. Operant conditioning of spinal reflexes: from basic science to clinical therapy. *Front Integr Neurosci* 8: 1–8, 2014.

Thompson RF. In search of memory traces. *Annu Rev Psychol* 56: 1–23, 2005.

Van Der Meulen JP, Gilman S. Recovery of muscle spindle activity in cats after cerebellar ablation. *J Neurophysiol* 28: 943–957, 1965.

Wang Y, Pillai S, Wolpaw JR, Chen XY. Motor learning changes GABAergic terminals on spinal motoneurons in normal rats. *Eur J Neurosci* 23: 141–150, 2006.

Wang Y, Pillai S, Wolpaw JR, Chen XY. H-reflex down-conditioning greatly increases the number of identifiable GABAergic interneurons in rat ventral horn. *Neurosci Lett* 452: 124–129, 2009.

Watanabe Y, Kinoshita K, Koguchi A, Yamamura M. A new method for evaluating motor deficits in 3-acetylpyridine treated rats. *J Neurosci Methods* 77: 25–29, 1997.

Welsh JP, Yamaguchi H, Zeng XH, Kojo M, Nakada Y, Takagi A, Sugimori M, Llina RR. Normal motor learning during pharmacological prevention of Purkinje cell long-term depression. *Proc Natl Acad Sci USA* 102: 17166–17171, 2005.

Wolpaw JR. The complex structure of a simple memory. *Trends Neurosci* 20: 588–594, 1997.

Wolpaw JR. What can the spinal cord teach us about learning and memory? *Neuroscientist* 16: 532–549, 2010.

Wolpaw JR, Chen XY. The cerebellum in maintenance of a motor skill: a hierarchy of brain and spinal cord plasticity underlies H-reflex conditioning. *Learn Mem* 13: 208–215, 2006.

Wolpaw JR, Chen XY. Operant conditioning of reflexes. In: *Encyclopedia of Neuroscience*, edited by Squire LR. Oxford, UK: Academic, 2009, vol. 7, p. 225–233.

Wolpaw JR, Herchenroder PA. Operant conditioning of H-reflex in freely moving monkeys. *J Neurosci Methods* 31: 145–152, 1990.

Wolpaw JR, Herchenroder PA, Carp JS. Operant conditioning of the primate H-reflex: factors affecting the magnitude of change. *Exp Brain Res* 97: 31–39, 1993.

Wolpaw JR, Lee CL. Memory traces in primate spinal cord produced by operant conditioning of H-reflex. *J Neurophysiol* 61: 563–572, 1989.

Wolpaw JR, Tennissen AM. Activity-dependent spinal cord plasticity in health and disease. *Annu Rev Neurosci* 24: 807–843, 2001.